Sound transmission through suspended ceilings beneath floors

Thomas Scelo (1) and C. Roger Halkyard (2)

(1) Marshall Day Acoustics Ltd, Auckland
t.scelo@auckland.ac.nz
(2) Department of Mechanical Engineering, University of Auckland, New Zealand
Private Bag 92019, Auckland

ABSTRACT

The insulation performances of floor/ceiling systems are yet to be fully understood as the mechanisms responsible for the transmission of sound are complex. An analytical model predicting the performances of such systems has been developped in order to develop and explain structures with improved insulation. The paper presents briefly the modelling approach and the accuracy of the predictions. The model, by focusing on the low frequencies range, employs a modal decomposition method. The solution relies neither on the periodicity of the stiffened ceiling panels or suspension system nor on the infinite extend of the floor. The quadratic vibration velocity of the ceiling panel is predicted. Comparisons are made between measurements and prediction.

INTRODUCTION

Suspended ceilings beneath floors are a very common solution to improve the sound insulation of a floor design even though not all phenomena involved are fully understood. In this paper, the analytical model used to predict the performances of such a structure is first presented as a set of equations governing either a vibration displacement field or a sound pressure field of a component of the structure. The solution to this problem is then presented before the numerical predictions are compared with measurement data.

ANALYTICAL MODEL

The frequency range considered in this study is 0 to 500Hz. The displacements and sound pressure fields are written as the sums of trigonometric functions (modeshapes) that describ the vibroacoustic states of each component. The unknowns of the problem are then the associated expansion coefficients which are obtained by writing the problem as a matrix equation.

Monolithic Floor

The monolithic floor considered in the present study is a single concrete slab of constant thickness h_1, Young's modulus E_1, density ρ_1 and corrected shear modulus G_1^* (Figure 1). It is modelled as a thick plate with general elastic boundary conditions defined, at each point of the perimeter, by a set of transverse and rotational springs.

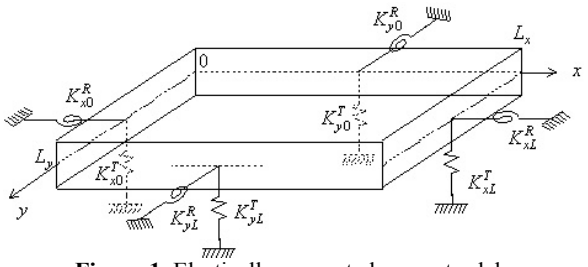

Figure 1. Elastically supported concrete slab.

The transverse displacement u_1 of the concrete floor can be expanded as

$$u_1(x,y) = \sum_{p,q=1}^{\infty} P_{pq}\Psi_p(x)\Theta_q(y), \qquad [1]$$

where P_{pq} are the expansion coefficients (unknowns to the problem). $\psi_p(x)$ and $\Theta_q(y)$ are the modeshapes, each is defined as the sum of the modeshape associated with a simply supported plate and a function of the stiffnesses of the springs at the boundaries (Timoshenko 1940, Li 2001). Finally, the transverse displacement field is the solution to the following governing equation

$$\sum_{p,q=1}^{\infty} P_{pq}\iint_S \psi_p^*\Theta_q^*\,\hat{D}_{pq}^{(1)}\,\psi_k\Theta_l\,dS = \iint_S \psi_k^*\Theta_l^*\,\hat{N}F\,dS, \qquad [2]$$

where $\hat{D}_{pq}^{(1)}$ and $\hat{N}F$ are respectively the operator associated with the governing equation for the transverse displacement of a thick plate and the associated non-homogeneous term (Skudrzyk, 1968). S is the surface area of the concrete floor. For a simply supported plate, the right hand side term of equation [2] becomes $\hat{D}_{pq}^{(1)}P_{pq}S/4$ and

$$\hat{D}_{pq}^{(1)} = D_1(\alpha_p^2+\beta_q^2)^2 - \omega\left[\frac{\rho_1 h_1^3}{12}+\frac{D_1\rho_1}{G_1^*}\right](\alpha_p^2+\beta_q^2) - \rho_1 h_1\omega^2\left[1-\omega^2\frac{\rho_1 h_1^2}{12G_1^*}\right], \qquad [3]$$

$$\hat{N}F = \left[1-\frac{D_1\Delta}{G_1^* h_1}-\omega^2\frac{\rho_1 h_1^2}{12G_1^*}\right]F(x,y), \qquad [4]$$

where $\alpha_p = p\pi/L_x$, $\beta_q = q\pi/L_y$ and where Δ is the bi-harmonic operator.

Suspension System

The suspension systems come in a variety of shapes and materials, connecting the concrete floor to the ceiling. The concrete floor to rod connection is typically rigid but can also include a damping rubber block. The connection at the other hand consists of a steel clip that can offer both resilience and damping. Additionaly, the ceiling batten can contribute significantly to the resilience of the suspension system depending on its shape (Figure 2).

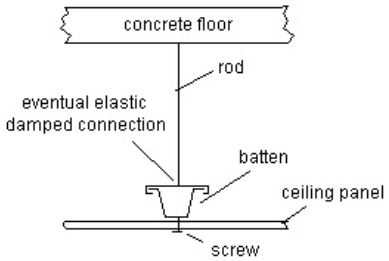

Figure 2. The suspension system.

The suspension rod in subjected to the forces and moments applied by the vibrating concrete floor and ceiling at its extremities and constitutes a main path of vibration transmission. The length, stiffnesses and density of such rod result in natural frequencies well above the 500Hz limit; the suspension system can therefore be modelled as a lumped system comprising of longitudinal and flexural springs and dampers, the combination of which is described by the equivalent dynamic stiffness Z_{eq}. If the suspension system consists of a longitudinal spring K_C, a flexural spring K_M and a damping C_R, then

$$Z_{eq} = K_C + j\omega C_R + K_M \Delta. \qquad [6]$$

Let u_2 denotes the transverse displacement field of the ceiling panel, the reaction force exerted by the suspension system on the concrete floor and suspended ceiling is a function of the transverse displacement difference and angular displacement difference between the two plates:

$$F_{rod} = Z_{eq}\left[u_1(x,y) - u_2(x,y)\right]\delta(x-x_\alpha)\delta(y-y_\beta), \qquad [5]$$

where (x_α, y_β) denotes the positions of the suspension rod.

Ceiling Panel

Ceiling panels generally consist of a single or double layer of gypsum board, stiffened by an array of ceiling battens and are, typically, supported by peripheral "L-shaped" channels (Figure 3). The array of battens is, in most cases, periodic. The model proposed here does not assume any periodicity in the battens' and rods' distributions so that the performances of a wider range of designs can be predicted. Unpublished measurement data has shown that the boundary conditions of the ceiling battens and ceiling panel, when screwed to the peripheral channel, are best modelled as simply supported, allowing for rotation but no transverse displacements.

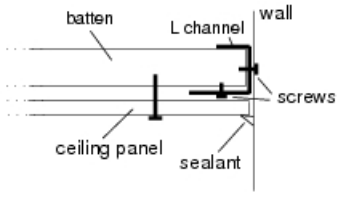

Figure 3. Boundary conditions for ceiling panel and battens

Typically, ceiling panels are periodically screwed to the array of battens. Unpublished data has shown that these screw connections are best modelled as rigid point connections when the bending wavelength in the panel is shorter than five times the screw spacing and as a rigid line connection otherwise. The reaction force exerted by the battens on the ceiling panel can then be written as $F_{bat} = \hat{H}\,u_2(x,y)\delta(x-x_b)\delta(y-y_s)$ with

$$\hat{H} = EI_y \frac{\partial^4}{\partial y^4} + GJ_y \frac{\partial^4}{\partial x^2 \partial y^2} - \omega^2 \rho_b \left(S_b - I_p \frac{\partial^2}{\partial x^2} \right), \qquad [7]$$

where EI_y and GJ_y are respectively the complex flexural and torsional stiffnesses, ρ_b is the density, S_b the cross-sectional area and I_p the polar moment of inertia of the battens; (x_b, y_s) are the coordinates of the screws. If the displacement field is decomposed in a basis of eigenfunctions $\varphi_p(x)\zeta_q(y)$ satisfying the boundary conditions above, and if the expansion coefficients are denoted C_{pq} so that

$$u_2(x,y) = \sum_{p,q=1}^{\infty} C_{pq}\varphi_p(x)\zeta_q(x), \qquad [8]$$

the equation governing the displacement field of the ribbed ceiling panel can be written as

$$\hat{D}_{pq}^{(2)} C_{pq}(S/4) = \sum_{\alpha,\beta} \iint_S F_{bat}\,\varphi_p\zeta_q dS + \sum_{r,s} \iint_S F_{rod}\,\varphi_p\zeta_q dS, \qquad [9]$$

where $\hat{D}_{pq}^{(2)} = \overline{D}_2(\alpha_p^2 + \beta_q^2)^2 - \rho_2 h_2 \omega^2$.

Cavity

Typically, the cavity is partly filled with a fibrous material for attenuation of the sound transmission from the floor to the ceiling panel via the air in the cavity. The partly filled cavity is modelled as two subsequent media of propagation (Figure 4). The vertical walls of the cavity are assumed impervious.

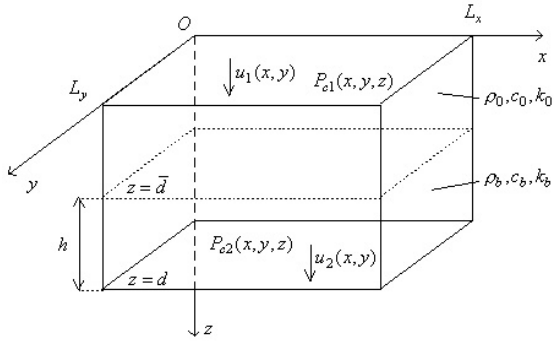

Figure 4. Cavity with infill, notations.

The first domain of propagation is defined by $0 \le z \le \overline{d}$ and the medium of propagation is air (characteristic impedance $\rho_0 c_0$, wavenumber $k_0 = \omega / c_0$). The second domain of propagation is defined by $\overline{d} \le 0 \le d$ and the medium of propagation is modelled as an equivalent dissipative fluid with the complex characteristic impedance Z_{fib} defined in (Delany & Bazley, 1970) as a function of the airflow resistivity σ of the fibrous material (Voronina 1996). The complex impedance results in a complex propagation constant k_{fib}. The two Helmholtz equations governing the sound pressure field in the sub-domains are respectively written as

$$[\Delta + k_0^2\,]p_{C1}(x,y,z) = 0, \quad \forall z \in [0,\bar{d}\,], \qquad [10]$$

$$[\Delta + k_{fib}^2]p_{C2}(x,y,z) = 0, \quad \forall z \in [\bar{d},d]. \qquad [11]$$

The conditions of continuity of the acoustic and mechanical velocities at the solid-fluid ($z = 0$) and fluid-solid ($z = d$) interfaces leads to relationships between the sound pressure fields in the cavity and the displacements u_1 and u_2 of the plates:

$$\left.\frac{\partial p_{C1}}{\partial z}\right|_{z=0} = \omega^2 \rho_0 u_1 \text{ and } \left.\frac{\partial p_{C2}}{\partial z}\right|_{z=d} = \omega^2 \rho_{fib} u_2 . \qquad [12]$$

Finally, the continuity of the particle velocity at the interface between the two media of propagation gives a direct relationship between the sound pressure fields (Bruneau & Scelo 2006)

$$\left.\frac{\partial p_{C2}}{\partial z}\right|_{z=\bar{d}} = \frac{\rho_{fib}}{\rho_0} \left.\frac{\partial p_{C1}}{\partial z}\right|_{z=\bar{d}} . \qquad [13]$$

The sound pressure fields is written as the summation over the acoustic modeshapes of the cavity, given as $\Phi_p(x)\Omega_q(x) = \cos[p\pi x / L_x]\cos[q\pi y / L_y]$, so that

$$p_{C1}(x,y,z) = \sum_{p,q} \xi_{pq}(z)\Phi_p(x)\Omega_q(y), \qquad [14]$$

$$p_{C2}(x,y,z) = \sum_{p,q} \lambda_{pq}(z)\Phi_p(x)\Omega_q(y), \qquad [15]$$

the substitution of equations [14] and [15] into equations [10] to [13] leads directly to the expressions for the sound pressure fields as functions of the expansion coefficients P_{pq} and C_{pq} of the plates' displacements.

Solution

The problem can now be fully defined by writing the equations governing the displacements of the floor and ceiling panel as

$$\begin{cases} \sum_{p,q=1}^{\infty} \hat{D}_{pq}^{(1)} P_{pq} \Psi_p(x)\Theta_q(y) = F_e \delta(x - x_e)\delta(y - y_e) - \sum_{\alpha,\beta=1}^{Nrod} F_{rod} \\ \qquad\qquad - p_{C1}(x,y,0) + p_S(x,y,0), \\ \sum_{p,q=1}^{\infty} \hat{D}_{pq}^{(2)} C_{pq} \varphi_p(x)\zeta_q(y) = \sum_{\alpha,\beta=1}^{Nrod} F_{rod} - \sum_{r,s=1}^{Nscrew} F_{bat} \\ \qquad\qquad + p_{C2}(x,y,d) - p_R(x,y,d). \end{cases} \qquad [16]$$

Multiplying the first equation of the system [16] by the modeshape $\Psi_k(x)\Theta_l(y)$ and the second equation by $\varphi_k(x)\zeta_l(y)$ and integrating over the surface areas of the floor defined by $S = \{0 \le x \le L_x, 0 \le y \le L_y\}$, before applying the orthogonality relationships between modeshapes leads to a new system of equations which, when written in a matrix form, becomes

$$\begin{aligned} &\left[\Lambda D^{(1)} + 4\Lambda\Theta + P_{C1/1} - P_S\right]\{P\} + \left[-4\Lambda\Theta + P_{C1/2}\right]\{C\} = 4\Lambda[B], \\ &-\left[4\Lambda\Theta + P_{C2/1}\right]\{P\} + \left[\Lambda D^{(2)} + 4\Lambda\Theta + H - P_{C2/2} + P_R\right]\{C\} = 0, \end{aligned} \qquad [17]$$

where $D^{(1)}$ and $D^{(2)}$ denote respectively the sums of the stiffness and inertia matrices associated with the free vibrations of the uncoupled floor and ceiling panel; Θ is the matrix associated with the finite sum of all local forces and moments applied by the rods, H denotes the matrix associated with the reaction force from the battens to the displacement of the ceiling panel, $P_{Ci/j}$ are the matrices of modal coupling terms between the i^{th} part of the cavity on the j^{th} plate and $[B]$ is the coupling matrix between the driving point force and the modal displacement of the floor. $\{P\}$ and $\{C\}$ are vectors, the components of which are respectively the expansion coefficients P_{pq} and C_{pq} . Finally, condensing the system of matrix equations [17] into a single equation

$$\begin{bmatrix} [\Lambda D^{(1)} + 4\Lambda\Theta + P_{C1/1} - P_S] & [-4\Lambda\Theta + P_{C1/2}] \\ -[4\Lambda\Theta + P_{C2/1}] & [\Lambda D^{(2)} + 4\Lambda\Theta + H - P_{C2/2} + P_R] \end{bmatrix} \begin{bmatrix} \{P\} \\ \{C\} \end{bmatrix} = \begin{bmatrix} 4\Lambda[B] \\ 0 \end{bmatrix}, \qquad [18]$$

leads, after inverstion of equation [18], to the expression of the expansion coefficients C_{pq} for the displacement of the ceiling panel. The vibration velocity of the ceiling panel is then directly reconstructed using equation [8]. The mean-square vibration velocity of the ceiling panel is directly available for a given harmonic point excitation force applied to the concrete floor (Cremer *et al.* 2005).

NUMERICAL RESULTS

Experimental Data

The system considered is shown in Figure 5, consisting of a 140mm concrete slab to which were rigidly connected an array of fifteen 180mm long steel rods. Five parallel battens were suspended from the array of rods, 600mm apart, before a sheet of 13mm gypsum was screwed to the battens. The screws were set at 200mm centres.

Figure 5. Array of battens suspended from a concrete floor before the installation of the ceiling panel.

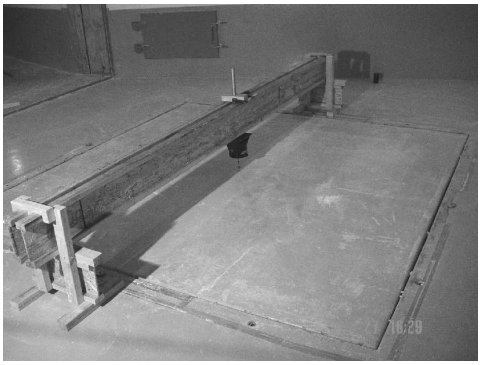

Figure 6. Electromagnetic shaker on the concrete floor.

The characteristics of the materials used for the measurement and simulations are given in Table 1. The same values were used for the prediction of the mobility.

Table 1. Characteristics of the materials

Concrete		*Ceiling*	
$E_1\,(\mathrm{Nm^{-2}})$	$29\ 10^9$	$E_2\,(\mathrm{Nm^{-2}})$	$2.8\ 10^9$
$h_1\,(\mathrm{mm})$	140	$h_2\,(\mathrm{mm})$	13
$\rho_1\,(\mathrm{kg\,m^{-3}})$	2400	$\rho_2\,(\mathrm{kg\,m^{-3}})$	700
Rods		*Battens*	
$E_c\,(\mathrm{Nm^{-2}})$	$210\ 10^9$	$E_y\,(\mathrm{Nm^{-2}})$	$210\ 10^9$
$\rho_c\,(\mathrm{kg\,m^{-3}})$	7500	$I_y\,(\mathrm{m^4})$	$11.9\,10^{-9}$
length (mm)	180	$J_y\,(\mathrm{m^4})$	$5\,10^{-12}$
radius (mm)	6	$\rho_b\,(\mathrm{kg\,m^{-3}})$	7500
		$S_b\,(\mathrm{m^2})$	$66\,10^{-6}$
Cavity		*Dimensions of system*	
σ (mks Rayls/m)	4135	$L_x\,(\mathrm{m})$	3.4
d (mm)	180	$L_y\,(\mathrm{m})$	3.4
$\bar{d}$ (mm)	105		

The harmonic point force was provided by a B&K4809 electromagnetic shaker driven with a random signal generated by a HP3566A dynamic signal analyser, amplified by a Ling TPO25 amplifer and mounted onto a rigid frame above the concrete slab. A PCB208C02 force transducer measured the excitation signal (Figure 6).

Two PCB352C68 accelerometers with PCB480E09 power supplies were used to measure the vibration acceleration of the suspended ceiling from which the transfer mobility of the whole system was derived. The acceleration signal was recorded over a period of 1 second and the averaged spectrum of the signal averaged over 128 repetitions of the measurement at 37 different positions over the surface area of the ceiling.

The space-averaged mobility of the system, equal to the normalised quadratic velocity of the ceiling panel, was estimated as

$$< H >= \frac{1}{|F|}\left[\frac{1}{S}\iint_S (j\omega u_2)^*(j\omega u_2)\,dS\right]^{1/2}, \qquad [18]$$

where * is the complex conjugate. The predicted and measured space-averaged mobilities are shown in Figure 7 for comparison.

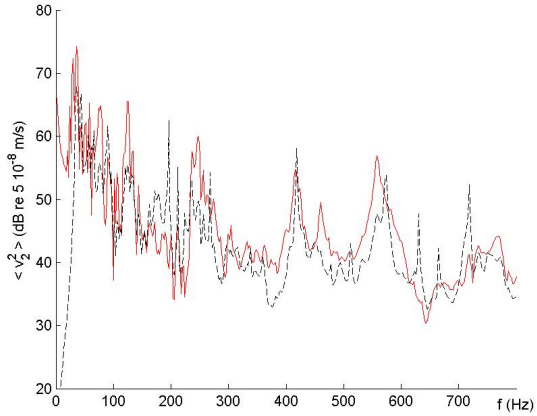

Figure 7. Measured (—) and predicted (− −) mobilities of the suspended ceiling.

Figure 7 shows that a good agreement has been found between the trend of the predicted and that of the measured mean-square velocity of the ceiling panel when the concrete floor is submitted to a harmonic point force excitation. The model predicts accurately the dominance of the resonance frequencies of the concrete floor at 250Hz, 430Hz and 560Hz. The overall magnitude of the response is in good agreement with that of the measured data.

CONCLUSION

In this paper, a model for predicting the dynamic response of a suspended ceiling beneath a floor was briefly presented. Limiting the analysis to the low frequency range, the modal decomposition of the displacement fields and sound pressure fields offers the benefit of isolating the different coupling terms between the different elements of the system.

The problem is simplified by combining the equations governing the displacement fields of the concrete floor and ceiling panel and that governing the sound pressure field in the cavity into a single matrix equation that can be numerically solved with a single matrix inversion.

It was shown that such a model can predict the dynamic response of a suspended ceiling beneath a floor with reasonable accuracy while offering a realistic approach by considering the finite size of the system, the elastic boundary conditions of the concrete floor, the partial filling of the cavity and the non-periodicity of the battens' and rods' distributions.

ACKLOWLEDGEMENTS

At the time of this investigation, the first author was affiliated to the Department of Mechanical Engineering, University of Auckland. This work was funded by the FoRST under the Technology Industry Fellowship scheme with the appreciated support of Winstone Wallboards Ltd.

REFERENCES

Bruneau M. & Scelo T. 2006, *Fundamentals of Acoustics*, ISTE Ltd, London.

Cremer L. Heckl M. & Petersson B. 2005, *Structure-borne Sound*, Springer, Berlin.

Delany M.E. & Bazley E.N. 1970, *Acoustical properties of fibrous absorbent material*, Applied Acoustics 3, p 105-116.

Li W.L. 2001, Vibration analysis of rectangular plates with general elastic boundary supports, Journal of Sound and Vibration 245(1), p 1-16.

Skudrzyk E. 1968, *Simple and complex vibratory systems*, The Pennsylvania State University Press, Park & London.

Timoshenko S. 1940, *Theory of plates and shells*, McGraw-Hill Book Company Inc., N.Y.

Voronina N. 1996, Improved empirical model of sound propagation through a fibrous material, Applied Acoustics 48, pp 121-132.